Modification of linear (β1→3)-linked gluco-oligosaccharides with a novel recombinant β-glucosyltransferase (trans-β-glucosidase) enzyme from Bradyrhizobium diazoefficiens

Dobruchowska, Justyna M; Jonsson, Jon O; Fridjonsson, Olafur H; Aevarsson, Arnthor; Kristjansson, Jakob K; Altenbuchner, Josef; Watzlawick, Hildegard; Gerwig, Gerrit J; Dijkhuizen, Lubbert; Kamerling, Johannis P

Published in:
Glycobiology

DOI:
10.1093/glycob/cww074

Publication date:
2016

Glycobiology, 2016, vol. 26, no. 11, 1157–1170
doi: 10.1093/glycob/cww074
Advance Access Publication Date: 21 September 2016
Original Article

OXFORD

Analytical Glycobiology

Modification of linear (β1→3)-linked gluco-oligosaccharides with a novel recombinant β-glucosyltransferase (*trans*-β-glucosidase) enzyme from *Bradyrhizobium diazoefficiens*

Justyna M Dobruchowska[2,†], Jon O Jonsson[3,†], Olafur H Fridjonsson[3], Arnthor Aevarsson[4], Jakob K Kristjansson[4], Josef Altenbuchner[5], Hildegard Watzlawick[5], Gerrit J Gerwig[2,6], Lubbert Dijkhuizen[2], Johannis P Kamerling[2,6], and Gudmundur O Hreggvidsson[1,3,7]

[2]Microbial Physiology, Groningen Biomolecular Sciences and Biotechnology Institute (GBB), University of Groningen, Nijenborgh 7, 9747 AG Groningen, The Netherlands, [3]Matís, Vínlandsleid 12, 113 Reykjavík, Iceland, [4]Prokazyme ehf. Vínlandsleid 10, 113 Reykjavík, Iceland, [5]Institut für Industrielle Genetik, Universität Stuttgart, Allmandring 31, 70569 Stuttgart, Germany, [6]NMR Spectroscopy, Bijvoet Center for Biomolecular Research, Utrecht University, Padualaan 8, 3584 CH Utrecht, The Netherlands, and [7]Department of Biology, University of Iceland, Sturlugata 7, 101 Reykjavík, Iceland

[1]To whom correspondence should be addressed: Tel: +354-4225047; Fax: +354-4225001; e-mail: gudmundur.o.hreggvidsson@matis.is

[†]These authors contributed equally to this work.

Received 16 December 2015; Revised 14 July 2016; Accepted 18 July 2016

Abstract

Recently, we have shown that glycoside hydrolases enzymes of family GH17 from proteobacteria (genera *Pseudomonas*, *Azotobacter*) catalyze elongation transfer reactions with laminari-oligosaccharides generating (β1→3) linkages preferably and to a lesser extent (β1→6) or (β1→4) linkages. In the present study, the cloning and characterization of the gene encoding the structurally very similar GH17 domain of the NdvB enzyme from *Bradyrhizobium diazoefficiens*, designated Glt20, as well as its catalytic properties are described. The Glt20 enzyme was strikingly different from the previously investigated bacterial GH17 enzymes, both regarding substrate specificity and product formation. The *Azotobacter* and *Pseudomonas* enzymes cleaved the donor laminari-oligosaccharide substrates three or four moieties from the non-reducing end, generating linear oligosaccharides. In contrast, the Glt20 enzyme cleaved donor laminari-oligosaccharide substrates two glucose moieties from the reducing end, releasing laminaribiose and transferring the remainder to laminari-oligosaccharide acceptor substrates creating only (β1→3)(β1→6) branching points. This enables Glt20 to transfer larger oligosaccharide chains than the other type of bacterial enzymes previously described, and helps explain the biologically significant formation of cyclic β-glucans in *B. diazoefficiens*.

Key words: *Bradyrhizobium diazoefficiens*, β-D-glucans, non-Leloir β-glucosyltransferase, oligosaccharide synthesis, structural analysis

Introduction

β-Glucans, made up of (β1→3)- and/or (β1→4)-linked D-glucopyranosyl residues, are important cell wall components of bacteria, fungi and plants, and as storage polysaccharides in seaweeds. Based on the presence/absence of other linkages, β-glucans can be further classified into various distinct types with different physicochemical properties. Thus, laminarin from seaweed has predominantly (β1→3) glycosidic linkages with (β1→6) branchings on every 10th glucose unit on average. On the other hand, β-glucans from barley, oat or wheat have mixed (β1→3) and (β1→4) linkages in the backbone, but no (β1→6) branching, and generally display higher molecular weights and viscosities (McIntosh et al. 2005).

The GH17 family glucoside hydrolases hydrolyze internal (β1→3) glycosidic linkages in β-glucan oligo- and polysaccharides. The family includes (β1→3)-glucan endohydrolases (EC 3.2.1.39), glucan (β1→3)-glucosidases (EC 3.2.1.58) and (β1→3)(β1→4)-glucan endohydrolases found in plants and fungi (CAZy database, http://www.cazy.org/GH17.html), and (β1→3)(β1→6)-*trans*-glucosidases originating from *Aspergillus fumigatus* (Mouyna et al. 1998; Gastebois et al. 2010), *Candida albicans* and *Saccharomyces cerevisiae* (Hartland et al. 1991; Goldman et al. 1995). GH17 enzymes have an apparent narrow phylogenetic distribution range in bacteria. They are common in *Proteobacteria* and *Bacteroidetes* with sporadic occurrences in other bacterial phyla.

GH17 enzymes in *Proteobacteria* appear to be involved in the synthesis of osmoregulated periplasmic β-glucans (OPGs), which are common constituents of their envelope. OPGs play a role in establishing symbiotic relationships between specific plant hosts and bacteria, such as *Agrobacterium tumefaciens* and *Bradyrhizobium diazoefficiens* USDA 110 previously classified as *Bradyrhizobium japonicum* USDA 110 (Bohin 2000; Delamuta et al. 2013). In other bacteria, such as *Pseudomonas syringae* and *Erwinia chrysanthemi*, they mediate similar plant host interactions but rather as harmful virulence factors in disease development (Mukhopadhyay et al. 1988; Talaga et al. 1994; Cogez et al. 2001). Other studies have indicated roles in antibiotic resistance and in formation of biofilms (Lequette et al. 2007; Mah et al. 2003; Sadovskaya et al. 2010).

Recently, we have described the non-Leloir *trans*-β-glucosylation activity of three GH17 enzymes from *Proteobacteria* on linear (β1→3)-linked gluco-oligosaccharides, i.e. Glt1 from *Pseudomonas aeruginosa* PAO1, Glt3 from *Pseudomonas putida* KT2440 and Glt7 from *Azotobacter vinelandii* ATCC BAA-1303 (Hreggvidsson et al. 2011). It was the first characterization of GH17 enzymes with *trans*-glucosylation activity from bacteria. All recombinant enzymes cleaved laminari-oligosaccharides (Lam-$Glc_{4–9}$) and derived alditols, preferably three or four residues from the non-reducing end depending on the enzyme used, and transferred the tri- or tetra-saccharides to the non-reducing end of laminari-oligosaccharide(-alditol) acceptor substrates. Depending on the enzyme and substrates (free or reduced) used, besides (β1→3)-elongation activity, (β1→6)- or (β1→4)-elongation or (β1→6)-branching activities were also detected.

The genes encoding the GH17 enzymes in *B. diazoefficiens* USDA 110, *ndvB* and *ndvC*, play a role in the formation of cyclic β-glucans with (β1→3), (β1→6)-linked glucosyl residues (Bhagwat et al. 1996). Disruption of the *ndvB* gene abolished the formation of cyclic (β1→3), (β1→6)-linked glucans and the resulting mutant strain was hypoosmotically sensitive and symbiotically ineffective (Bhagwat and Keister 1995). Disruption of the *ndvC* gene led to the synthesis of altered cyclic (β1→3)-glucans composed of almost entirely (β1→3) linkages. The resulting mutant strain was only slightly sensitive to hypoosmotic growth conditions compared with the *ndvB* mutant, but impaired in symbiotic interactions with soybean (Bhagwat et al. 1996). In another study, insertional inactivation of a homologous gene, *ndvB* in *P. aeruginosa*, revealed a role in the biosynthesis of cyclic (β1→3)-glucans (Sadovskaya et al. 2010). None of these putative GH17 *trans*-β-glucosidase enzymes have been characterized.

In this paper, we report the characterization of the GH17 domain of the NdvB *trans*-β-glucosidase from *B. diazoefficiens*, here designated as Glt20. The activity of the recombinant enzyme Glt20 was investigated by using linear (β1→3)-linked gluco-oligosaccharides (laminari-oligosaccharides; Lam-Glc_{2-10}) as donor/acceptor substrates. Thin-layer chromatography (TLC), matrix-assisted laser desorption ionization time-of-flight mass spectrometry (MALDI-TOF-MS), one- and two-dimensional ^{1}H and ^{13}C nuclear magnetic resonance (NMR) spectroscopy, and high-pH anion-exchange chromatography (HPAEC) were used to characterize formed oligosaccharide products. Despite significant sequence and structural similarity, our study shows that Glt20 is distinctly different in substrate specificity and product formation from the Glt1, Glt3 and Glt7 homologues previously described (Hreggvidsson et al. 2011). This study includes the first characterization of a bacterial *trans*-β-glucosidase that solely generates (β1→6) branches, using laminari-oligosaccharide as substrate.

Results

Production and purification of recombinant Glt20

The *B. diazoefficiens* GH17 protein domain, denoted Glt20, was produced as a fusion protein (MalE-6xHis-Smt3-Glt20) by applying the pJOE4905/*Escherichia coli* BL21 C43 expression system. High expression levels (yields of 20–30% of total soluble proteins in crude extract) were only achieved when the GH17 domain was fused to the *E. coli* maltose binding protein (MalE). The fused protein had a 6xHis tag that facilitated its efficient purification. Figure 1 shows the sodium dodecyl sulfate-polyacrylamide gel electrophoresis (SDS-PAGE) profiles and indicates the size of the different forms of the cloned Glt20 enzyme going from crude extract to final product. After purification of the crude extract on an amylose column, making use of the MalE domain (Figure 1, lane 3), the recombinant fusion protein (calculated molecular mass 87.8 kDa) was cleaved by ULP protease (Figure 1, lane 4) into proteins of molecular mass less than 34 kDa and close to 55 kDa according to the SDS-PAGE run profile, affiliated with the Glt20 (calculated mass 31.5 kDa) and the MalE-6xHis-Smt3 fragment (calculated mass 53.6 kDa), respectively. The proteins were separated on a HisTrapFF chelating column, whereby the MalE-6xHis-Smt3 protein was bound and the Glt20 enzyme eluted (data not shown). Glt20 was used in the following activity studies.

Activity screening of Glt20 on substrate oligosaccharides (Lam-Glc_2 - Lam-Glc_{10})

Solutions of the substrates laminaribiose (Lam-Glc_2) up to laminaridecaose (Lam-Glc_{10}) in 0.5 M KH_2PO_4/K_2HPO_4 buffer, pH 6.5 (determined as the optimal pH for the *trans*-β-glucosidase activity of Glt20 – data not shown), were individually incubated with Glt20 (1 mg/mL) at 30°C. As is evident from the thin-layer chromatogram in Figure 2, the enzyme was not active with Lam-Glc_2, Lam-Glc_3 and Lam-Glc_4. However, with Lam-Glc_5 to Lam-Glc_{10},

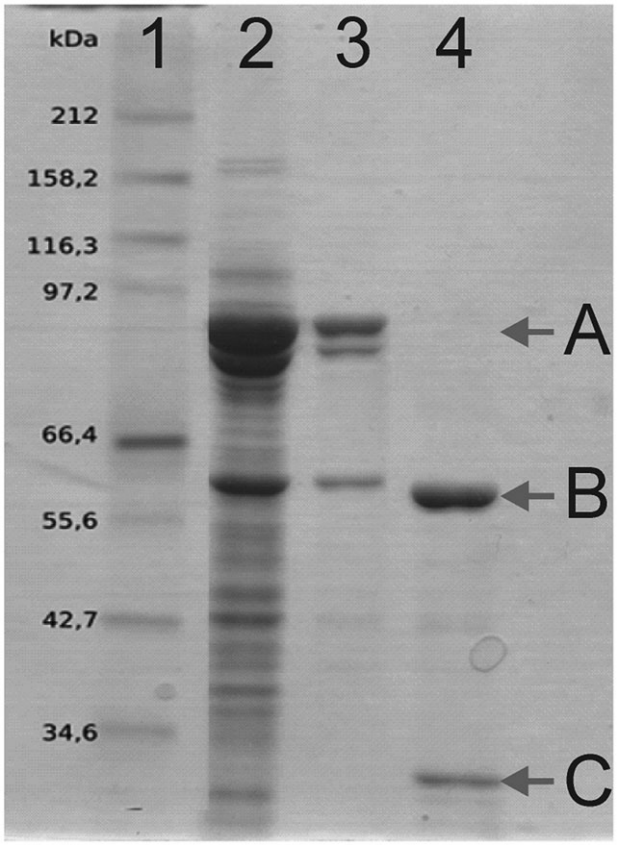

Fig. 1. Ten percent SDS-PAGE profiles of the different forms of the Glt20 enzyme during the purification steps. (1) Protein standard; (2) MalE-6xHis-Smt3-Glt20 crude extract sample before purification on an amylose column; (3) MalE-6xHis-Smt3-Glt20 sample after purification on an amylose column; (4) Sample after cleavage with ULP protease into MalE-6xHis-Smt3 and Glt20. The arrows point to the following bands: (A) MalE-6xHis-Smt3-Glt20 protein (Glt20-MalE); (B) MalE-6xHis-Smt3 fragment; (C) Glt20 enzyme (Glt20).

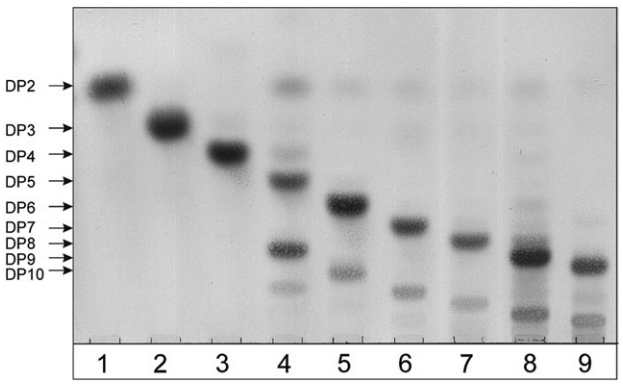

Fig. 2. TLC analysis of oligosaccharide mixtures generated after 24 h of incubation of (β1→3)-gluco-oligosaccharides (Lam-Glc_2 - Lam-Glc_{10}) with the Glt20 enzyme.

trans-glucosylation activity was observed, in each case indicated by TLC product bands above and below the substrate (formation of smaller and larger oligosaccharides as a result of a disproportionation reaction). In each of these cases laminaribiose (Lam-Glc_2) was clearly formed (Figure 2).

MALDI-TOF-MS analysis after 48 h of incubation (Figure 3) revealed that the most intensive transfer products (generally indicated as products with bruto formula Pro-Glc_x) formed are (a) from Lam-Glc_5: Pro-Glc_8, Pro-Glc_{11}, Pro-Glc_{14}; (b) from Lam-Glc_6: Pro-Glc_{10}, Pro-Glc_{14}, Pro-Glc_{18}; (c) from Lam-Glc_7: Pro-Glc_{12}, Pro-Glc_{17}; (d) from Lam-Glc_8: Pro-Glc_{14}, Pro-Glc_{20}; (e) from Lam-Glc_9: Pro-Glc_{16}, Pro-Glc_{23}; and (f) from Lam-Glc_{10}: Pro-Glc_{18}, Pro-Glc_{26}. So, Glt20 mainly catalyzes the transfer of oligosaccharides as big as Lam-Glc_{3-8} (depending on the size of the donor substrate) from the donor substrate to an acceptor oligosaccharide, with each substrate also resulting in Lam-Glc_2 formation. Only minor amounts of hydrolysis products were observed in the mass spectra after 48 h of incubation, but prolonged incubation up to 72 h resulted in an increased release of short saccharides of different sizes.

The Glt20 enzyme revealed no activity with the corresponding laminari-oligosaccharide-alditols Lam-Glc_2-ol - Lam-Glc_{10}-ol (data not shown). Taking together the results for the free and reduced oligosaccharides, it is clear that the action of Glt20 with the free laminari-oligosaccharides Lam-Glc_5 up to Lam-Glc_{10} results in a release of laminaribiose from the reducing end of the donor substrate, followed by a transfer of the remaining part to a second molecule of the substrate now functioning as an acceptor. This reaction repeatedly occurs, thus also resulting in synthesis of larger size oligosaccharides. In order to get detailed information about the structures of the formed products, semi-preparative-scale incubations were performed with Lam-Glc_5 and Lam-Glc_6.

Analysis of the saccharide mixture generated after 48 h of incubation of Lam-Glc_5 with Glt20

Laminaripentaose (Lam-Glc_5) (100 µL; 6.25 mg/mL) was incubated with Glt20 (70 µL; 1 mg/mL) in 0.5 M potassium phosphate buffer, pH 6.5 (30 µL) for 48 h at 30°C. MALDI-TOF-MS analysis of the incubation mixture mainly showed quasi-molecular ions $[M+K]^+$ at *m/z* 867.2, corresponding to the substrate Lam-Glc_5, and *m/z* 1353.5, *m/z* 1839.8 and *m/z* 2326.3, corresponding to products with the bruto formulae Pro-Glc_8, Pro-Glc_{11} and Pro-Glc_{14}, respectively (Figure 3A). The one-dimensional ^{1}H NMR spectrum of this mixture is shown in Supplementary data, Figure S1. See also Table I for NMR data of relevant β-D-gluco-oligosaccharides. The amount of oligosaccharides of DP >5 formed, mainly consisting of Pro-$Glc_{8,11,14}$, was estimated to be about 60% of total (based on MS peak intensities).

The saccharide mixture was fractionated on Bio-Gel P-2, and fractions of 5 min were collected and screened by TLC and MALDI-TOF-MS (data not shown). The two major carbohydrate-containing fractions A and B were further investigated. The MALDI-TOF mass spectrum of fraction A (Supplementary data, Figure S2a) showed one major quasi-molecular ion $[M+Na]^+$ at *m/z* 1337.4, corresponding to Pro-Glc_8, and very minor peaks (intensity ~5%) for Pro-Glc_7 (*m/z* 1175.1) and Pro-Glc_9 (*m/z* 1499.6). The MALDI-TOF mass spectrum of fraction B (Supplementary data, Figure S2b) showed one major quasi-molecular ion $[M+Na]^+$ at *m/z* 1823.9, corresponding to Pro-Glc_{11}, and minor peaks (intensity ~15%) for Pro-Glc_{10} (*m/z* 1661.2) and Pro-Glc_{12} (*m/z* 1985.3). The amounts of the minor products present in both fractions were too low for detection by NMR spectroscopy.

The one-dimensional ^{1}H NMR spectra of Pro-Glc_8 and Pro-Glc_{11} were very similar (Figure 4A and B); the same held for their two-dimensional NMR spectra. For the assignment of the various

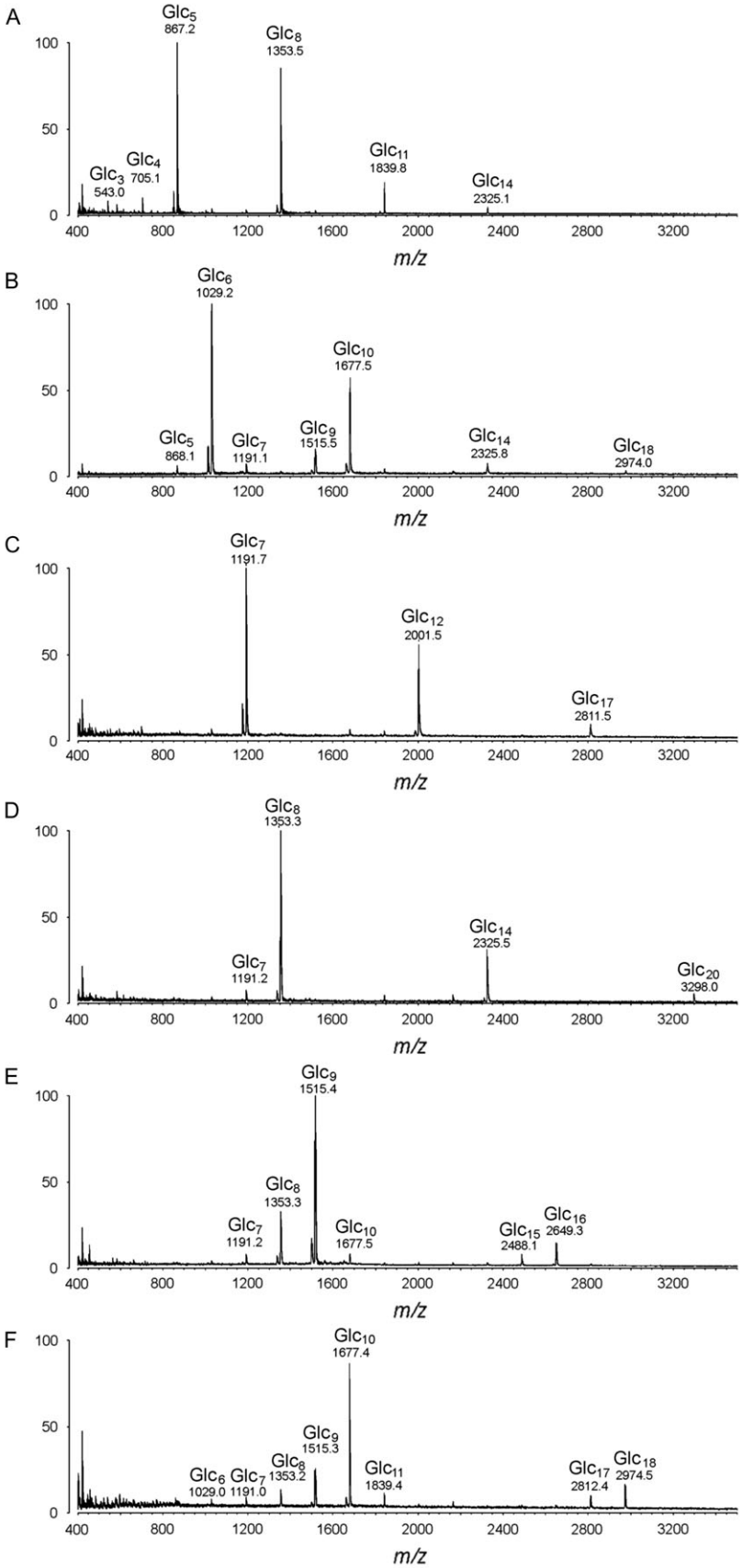

Fig. 3. MALDI-TOF mass spectra showing the quasi-molecular ions $[M+K]^+$ of the oligosaccharide mixtures, generated after 48 h of incubation of (A) Lam-Glc_5, (B) Lam-Glc_6, (C) Lam-Glc_7, (D) Lam-Glc_8, (E) Lam-Glc_9 and (F) Lam-Glc_{10} with the Glt20 enzyme.

Table I. ^{1}H and ^{13}C NMR chemical shifts[a] of glucose and glucitol (after reduction with $NaBH_4$) residues in oligosaccharide products obtained after incubation of (β1→3)-gluco-oligosaccharides (laminari-oligosaccharides) with the Glt20 and Glt20-MalE enzymes, recorded in D_2O at 335 K

Residue	H-1(a/1b) C-1	H-2 C-2	H-3 C-3	H-4 C-4	H-5 C-5	H-6a/H-6b C-6
Gα	5.240	3.72	3.91	3.52	3.88	3.84/3.76
-(1→3)-α-D-Glc*p*	93.1	72.0	83.4	69.2	72.3	61.8
Gβ	4.673	3.44	3.73	3.52	3.49	3.90/3.71
-(1→3)-β-D-Glc*p*	96.7	74.9	85.7	69.2	76.6	61.8
G2$_{\alpha}$	4.747	3.56	3.78	3.54	3.52	3.93/3.74
-(1→3)-β-D-Glc*p*-(1→3)-α-D-Glc*p*	103.7	74.3	85.3	69.1	76.7	61.7
G2$_{\beta}$	4.765	3.56	3.78	3.53	3.53	3.93/3.74
-(1→3)-β-D-Glc*p*-(1→3)-β-D-Glc*p*	103.7	74.3	85.3	69.1	76.7	61.7
Gi	4.785	3.56	3.78	3.54	3.52	3.93/3.74
-(1→3)-β-D-Glc*p*-(1→3)-	103.4	73.9	85.5	69.1	76.6	61.7
Gt	4.739	3.37	3.54	3.43	3.49	3.92/3.73
β-D-Glc*p*-(1→3)-	103.7	74.4	76.6	70.6	76.8	61.7
GA	4.517	3.33	3.51	3.41	3.46	3.92/3.74
β-D-Glc*p*-(1→6)-	103.6	74.0	76.7	70.7	76.8	61.8
GB	4.713	3.39	3.55	3.48	3.67	4.20/3.87
-(1→6)-β-D-Glc*p*-(1→3)-	103.6	74.4	76.5	70.5	75.5	69.5
GC	4.550	3.53	3.74	3.51	3.50	3.92/3.75
-(1→3)-β-D-Glc*p*-(1→6)-	103.5	73.6	85.6	69.1	76.6	61.6
GD	4.753	3.60	3.79	3.58	3.71	4.21/3.89
-(1→3,6)-β-D-Glc*p*-(1→3)-	103.5	74.0	85.4	69.1	75.4	69.5
G-ol	3.85/3.67	4.02	4.06	3.90	3.68	3.79/3.69
-(1→3)-D-Glc-ol	63.7	73.5	79.6	71.7	71.4	62.9
G2	4.675	3.59	3.78	3.53	3.52	3.94/3.74
-(1→3)-β-D-Glc*p*-(1→3)-D-Glc-ol	103.9	74.0	85.5	69.1	76.6	61.7

[a]In ppm relative to the signal of internal acetone (δ 2.225 for ^{1}H, δ 31.07 for ^{13}C).

signals, our earlier developed library of NMR data of Lam-Glc$_{2\text{-}10}$(-ol) was used (Table I) (Hreggvidsson et al. 2011). Both spectra show the anomeric signals **Gt**, **Gi**, **G2$_{\alpha/\beta}$** and **Gα/β**, belonging to linear (β1→3)-linked gluco-oligosaccharides: **Gt**, β-D-Glc*p*-(1→3)-; **Gi**, -(1→3)-β-D-Glc*p*-(1→3)-; **G2$_{\alpha/\beta}$**, -(1→3)-β-D-Glc*p*-(1→3)- (next to reducing-end **Gα/β**); **Gα/β**, -(1→3)-D-Glc*p*. The anomeric protons of the reducing-end glucose unit (**Gα** and **Gβ**) are at δ 5.240 (H-1α) and δ 4.673 (H-1β), respectively. The β-anomeric signal of the glucose unit **G2** is split into two doublets (δ 4.747, H-1$_{\alpha}$ / δ 4.765, H-1$_{\beta}$). The H-1 of the terminal glucose unit **Gt** is present at δ 4.739, overlapping with H-1$_{\alpha}$ of **G2**. The doublet resonating at δ 4.785 is stemming from the H-1's of the internal glucose units **Gi**. The two anomeric signals **GC** H-1 and **GD** H-1 observed at δ 4.550 and δ 4.753, respectively, together with a doublet signal at δ 4.21 (**GD** H-6a), indicate the presence of (β1→6) linkages. Residue **GC** is identified as a -(1→3)-β-D-Glc*p*-(1→6)- unit, and residue **GD** (overlapping with **Gi**, **Gt**, **G2$_{\alpha/\beta}$**) as a branching -(1→3,6)-β-D-Glc*p*-(1→3)- residue. The chemical shifts of the various residues were confirmed by two-dimensional NMR spectroscopy (TOCSY, ROESY and HSQC). Comparison of spectral peak-area ratios confirms that fractions A and B correspond to Pro-Glc$_8$ and Pro-Glc$_{11}$, respectively. Integration of the well-resolved anomeric signals of **GC**, **Gα/β** and the overlapping anomeric signals of **Gi**, **GD**, **Gt**, **G2$_{\alpha/\beta}$** in both spectra learns that Pro-Glc$_8$ contains one branching point [peak area ratio **Gα/β**:**GC**:(**Gi**,**GD**,**Gt**,**G2$_{\alpha/\beta}$**) = 1:1:6] and Pro-Glc$_{11}$ two branching points [peak area ratio **Gα/β**:**GC**:(**Gi**,**GD**, **Gt**,**G2$_{\alpha/\beta}$**) = 1:2:8]. A detailed NMR analysis of the isomeric structures of Pro-Glc$_8$ and Pro-Glc$_{11}$ is presented in the Supplementary data and summarized after the section "Analysis of the saccharide mixture generated after 72 h of incubation of Lam-Glc$_5$ with Glt20".

Analysis of the saccharide mixture generated after 72 h of incubation of Lam-Glc$_5$ with Glt20

Incubation of laminaripentaose (Lam-Glc$_5$) with Glt20 for 72 h at 30°C and pH 6.5 afforded a mixture of compounds different from that obtained after 48 h of incubation. Now, the MALDI-TOF mass spectrum showed compounds with quasi-molecular ions $[M+K]^+$ at *m/z* 705.5, 867.1, 1029.4, 1191.5, 1353.7, 1515.9 and 1678.0, corresponding to Pro-Glc$_4$, Lam/Pro-Glc$_5$, Pro-Glc$_6$, Pro-Glc$_7$, Pro-Glc$_8$, Pro-Glc$_9$ and Pro-Glc$_{10}$, respectively (Figure 5). One- and two-dimensional NMR analysis of the complete mixture of reaction products suggested that only linear gluco-oligosaccharides, containing (β1→3) and (β1→6) linkages, are present: **Gt**, β-D-Glc*p*-(1→3)-; **GA**, β-D-Glc*p*-(1→6)-; **Gi**, -(1→3)-β-D-Glc*p*-(1→3)-; **G2$_{\alpha/\beta}$**, -(1→3)-β-D-Glc*p*-(1→3)- (next to reducing-end **Gα/β**); **GB**, -(1→6)-β-D-Glc*p*-(1→3)-; **GC**, -(1→3)-β-D-Glc*p*-(1→6)-; **Gα/β**, -(1→3)-D-Glc*p* (Table I) (Hreggvidsson et al. 2011) (Supplementary data, Figure S3: one-dimensional ^{1}H NMR and 200-ms two-dimensional TOCSY spectra).

The saccharide mixture of the 72-h incubation was fractionated on Bio-Gel P-2, and fractions of 5 min were collected and screened by TLC and MALDI-TOF-MS (data not shown). The major carbohydrate-containing fractions C, D and E were further analyzed. The MALDI-TOF mass spectra (Supplementary data, Figure S4) of fractions C, D and E showed major quasi-molecular ions $[M+K]^+$ at *m/z* 705.1 (Pro-Glc$_4$), *m/z* 867.2 (Lam/Pro-Glc$_5$) and *m/z* 1029.4 (Pro-Glc$_6$), respectively. The minor products

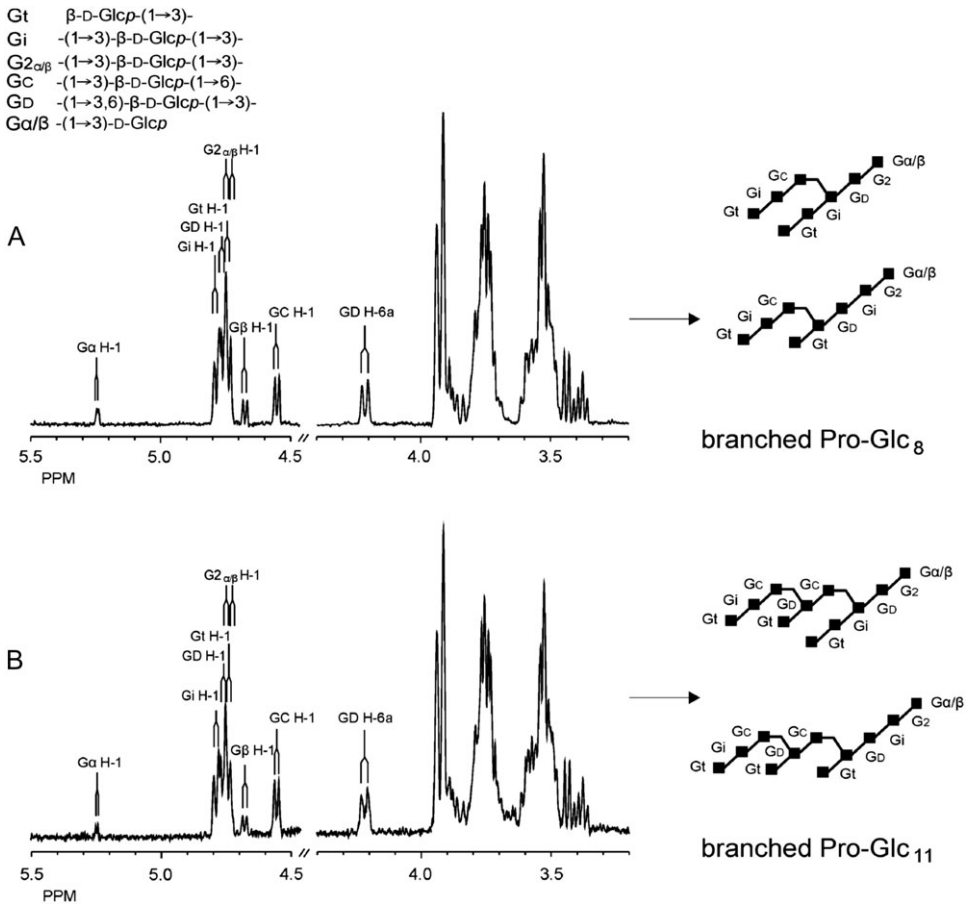

Fig. 4. One-dimensional ^{1}H NMR spectra (D_2O, 335 K) of (A) Pro-Glc_8 and (B) Pro-Glc_{11}, found in the oligosaccharide mixture after incubation of Lam-Glc_5 with the Glt20 enzyme for 48 h (pH 6.5, 30°C).

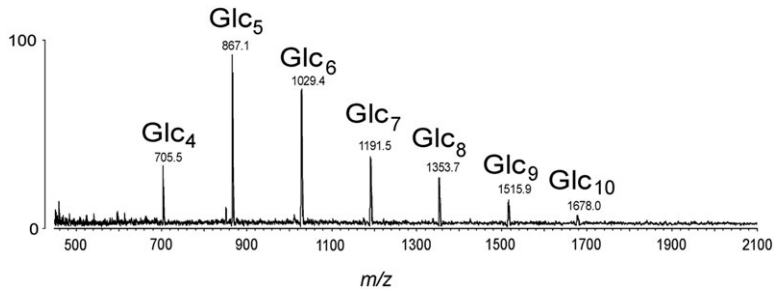

Fig. 5. MALDI-TOF mass spectrum showing the quasi-molecular ions $[M+K]^+$ of the oligosaccharide mixture, generated after 72 h of incubation of Lam-Glc_5 with the Glt20 enzyme.

(<10%) present in the three fractions were below the detection limits for NMR analysis.

The one-dimensional ^{1}H NMR spectra of Pro-Glc_4 (Figure 6A) and Pro-Glc_5 (Figure 6B) are very similar, showing the anomeric signals of **GA**, **GB**, **G2α/β** and **Gα/β** residues for Pro-Glc_4 and the anomeric signals of **GA**, **GB**, **Gi**, **G2α/β** and **Gα/β** residues for Pro-Glc_5 (Table I). The anomeric protons of the reducing-end glucose unit (**Gα** and **Gβ**) are detected at δ 5.240 (H-1α) and δ 4.673 (H-1β), respectively, and those of **G2α/β** at δ 4.747 (H-1_α) and δ 4.765 (H-1_β). The H-1 resonances of the internal residue **GB** and the terminal residue **GA** are found at δ 4.713 and δ 4.517, respectively. The ^{1}H NMR spectrum of Pro-Glc_5 contains an extra internal **Gi** residue with its H-1 signal at δ 4.785 (Hreggvidsson et al. 2011). For Pro-Glc_4 the spectral peak area ratio of **Gα/β:G2α/β:GA:GB** is 1:1:1:1, and for Pro-Glc_5 the spectral peak area ratio of **Gα/β:G2α/β:GA:GB:Gi** is 1:1:1:1:1. Based on the MS and NMR data, the following structures can be formulated for Pro-Glc_4 and Pro-Glc_5:

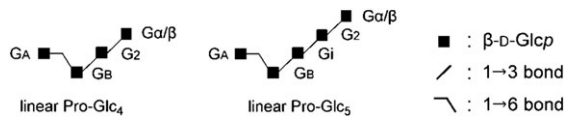

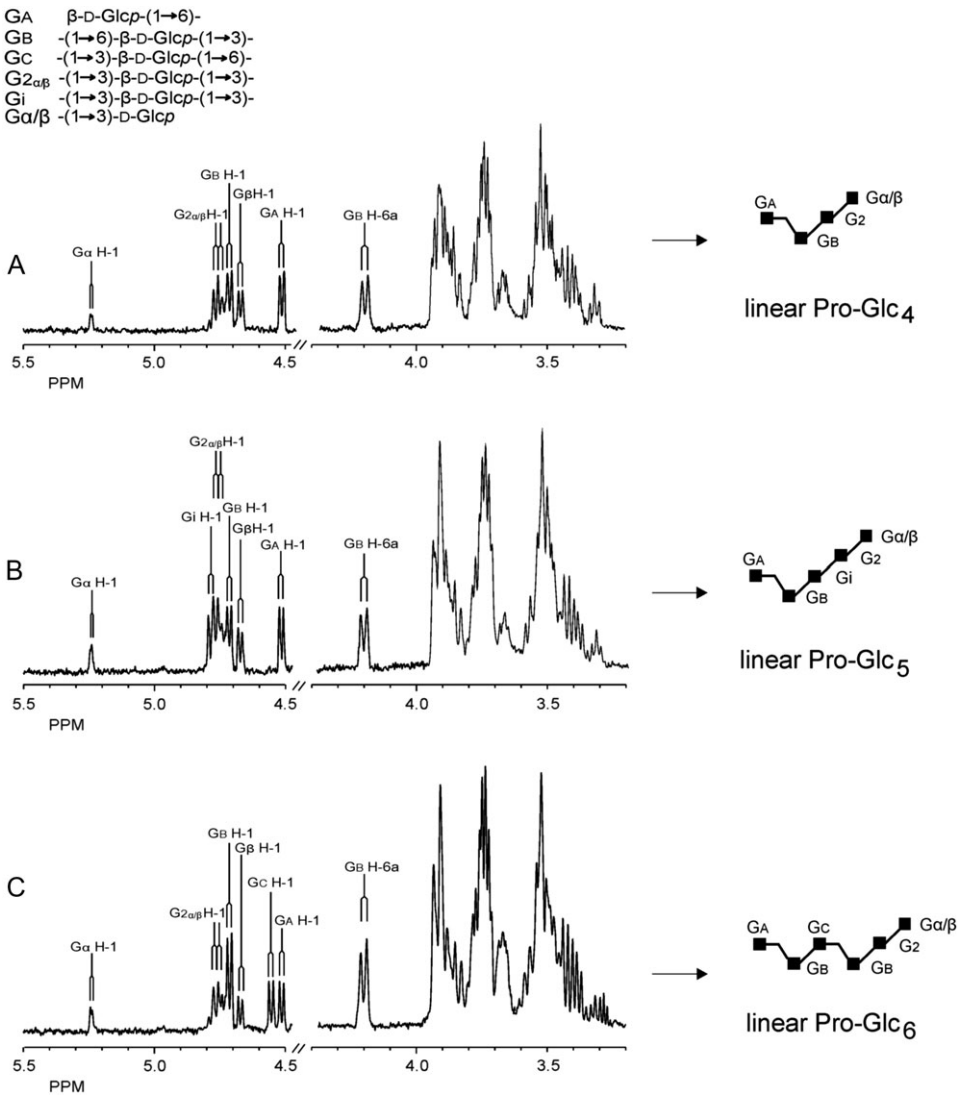

Fig. 6. One-dimensional ^{1}H NMR spectra (D_2O, 335 K) of (A) Pro-Glc_4, (B) Pro-Glc_5 and (C) Pro-Glc_6, found in the oligosaccharide mixture after incubation of Lam-Glc_5 with the Glt20 enzyme for 72 h (pH 6.5, 30°C).

In the one-dimensional ^{1}H NMR spectrum of Pro-Glc_6 (Figure 6C), one extra anomeric signal is observed at δ 4.550, assigned to an internal **G**C residue (Table I) (Hreggvidsson et al. 2011). Taking into account the spectral peak area ratio of **Gα/β**:**G2$_{α/β}$**:**G**A:**G**B:**G**C (1:1:1:2:1), the following structure can be formulated for Pro-Glc_6:

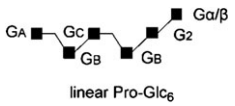

The characterization of these linear oligosaccharides was of utmost importance for the formulation of the structural isomers of Pro-Glc_8 and Pro-Glc_{11} (see Supplementary data for analytical details and its summary in the next section). The recombinant Glt20 enzyme was purified from *E. coli* BL21 crude extract. It should be noted that incubation of the *E. coli* BL21 crude lysate without the recombinant enzyme with Lam-Glc_3 up to Lam-Glc_6 for 72 h did not result in degradation products (data not shown). Further, no indication of co-purified β-1,3-glucosidase was observed. The formation of Pro-$Glc_{4,5,6}$ must therefore be the result of the hydrolytic activity of Glt20 enzyme on branched products when the linear oligosaccharide is depleted.

Characterization of the isomeric structures of Pro-Glc_8 and Pro-Glc_{11}

As an example for the rationalization behind the interpretation of the various ^{1}H and ^{13}C NMR assignments by two-dimensional TOCSY, ROESY and ^{13}C-^{1}H HSQC experiments, the analysis of Pro-Glc_8 is worked out in detail and shown in the Supplementary data, including the one-dimensional ^{1}H NMR and two-dimensional TOCSY (200 ms) spectra, and relevant parts of the two-dimensional ROESY (200 ms) and HSQC spectra of Pro-Glc_8 (Figure S5). The same detailed analysis was performed on Pro-Glc_{11} (data not shown). The ^{1}H and ^{13}C chemical shifts of the **Gt**, **Gi**, **G2$_{α/β}$**, **G**C, **G**D and **Gα/β** glucose residues are listed in Table I.

Based on the MS and NMR data collected for Pro-Glc_8 and Pro-Glc_{11}, combined with the MS and NMR data of the products

formed after 72 h of incubation (removal of β-D-Glc*p*-(1→3)- residues, due to hydrolytic activity of Glt20), the following molecular structures for Pro-Glc_8 and Pro-Glc_{11} are proposed to be present:

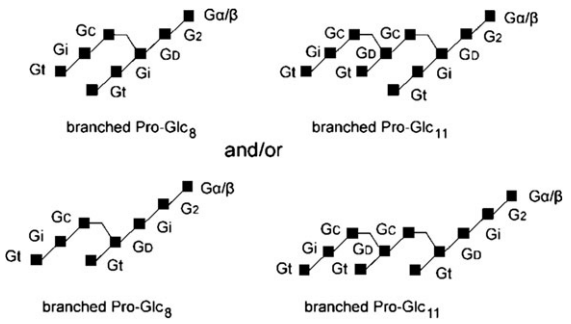

Taking together, it appears that the two Pro-Glc_8 oligosaccharides are synthesized by a transfer of a β-D-Glc*p*-(1→3)-β-D-Glc*p*-(1→3)-β-D-Glc*p*- trisaccharide unit from the non-reducing end of a donor Lam-Glc_5 substrate to the third or fourth internal Glc residue of an acceptor Lam-Glc_5 substrate via an O-3→O-6 transition, thereby releasing laminaribiose (first branching). Then, the formed Pro-Glc_8 oligosaccharides are used as acceptor substrates for transfer of another β-D-Glc*p*-(1→3)-β-D-Glc*p*-(1→3)-β-D-Glc*p*- trisaccharide unit from the non-reducing end of a donor Lam-Glc_5 substrate, but now to O-6 of the internal Glc residue of the trisaccharide branch introduced in the first step to yield the two Pro-Glc_{11} oligosaccharides (second branching). Along the same line of reasoning, the minor amount of Pro-Glc_{14}, seen in the MALDI-TOF mass spectrum (Figure 3A) is the result of a transfer of a third β-D-Glc*p*-(1→3)-β-D-Glc*p*-(1→3)-β-D-Glc*p*- trisaccharide unit (third branching), in a similar way as mentioned for the second branching. Taking into account that after 72 h of incubation no indications were found for the presence of stripped structures with two branches next to each other, such structures are not assumed for Pro-Glc_8, Pro-Glc_{11} and Pro-Glc_{14} (see next section).

HPAEC/NMR analysis of oligosaccharide-alditols obtained by incubation of Lam-Glc_5 with Glt20, followed by reduction with $NaBH_4$

To unravel the mixture of products after incubation of Lam-Glc_5 with Glt20 in more detail, also in terms of incubation time, a separation by HPAEC on Carbo-Pac PA-1 was preferred over a Bio-Gel P-2 fractionation. However, to make the oligosaccharide mixtures, obtained after incubation, suitable for such a profiling, the oligosaccharides were first converted into their corresponding oligosaccharide-alditols by reduction with $NaBH_4$. In this way, the possibility of peeling reactions at high pH, due to the presence of (1→3) linkages in the free oligosaccharides, were avoided. Note that Lam-Glc_5-ol itself is not a donor substrate for the enzyme (see above).

In Figure 7, the HPAEC profiles of the oligosaccharide-alditol mixtures obtained via incubation of Lam-Glc_5 with Glt20 for 0, 12, 24, 48 and 72 h (pH 6.5, 30°C) and subsequent reduction are depicted, showing the formation of a series of products up to DP11. Most of the alditol products formed within 72 h (included in Figure 7) were isolated and investigated by MALDI-TOF-MS and one- and two-dimensional NMR spectroscopy. As a few examples, the one-dimensional ^{1}H NMR spectra of Pro-Glc_4-ol, Pro-Glc_5-ol and Pro-Glc_8-ol [peak area ratio **G2:Gc:(Gi,GD, Gt)** = 1:1:5] are shown in Supplementary data, Figure S6. After 12 h, the two co-eluting branched products corresponding with Pro-Glc_8 (peaks 5 and 5′) and the two co-eluting branched products corresponding with Pro-Glc_{11} (peaks 6 and 6′) are already seen in the profile. But the five profiles also give a good impression about the consecutive hydrolysis of terminal β-D-Glc*p*-(1→3)- residues that takes place, converting branched structures into linear structures, keeping (β1→6) linkages intact. It can be deduced that prolonged incubation resulted in a decrease in molecular size of the products and the complete disappearance of the Lam-Glc_5 substrate.

Activity of the Glt20 enzyme on Lam-Glc_6

Laminarihexaose (Lam-Glc_6) was incubated with the Glt20 enzyme for different times at 30°C and pH 6.5. The formed saccharide mixtures were investigated using TLC, MALDI-TOF mass spectrometry, HPAEC and NMR spectroscopy. In the following some relevant results are summarized.

The MALDI-TOF mass spectrum (Figure 3B) of the saccharide mixture obtained after 48 h of incubation of Lam-Glc_6 with Glt20 showed major quasi-molecular ions $[M+K]^+$ at *m/z* 1029.2, corresponding to the substrate Lam-Glc_6, and *m/z* 1677.5, corresponding to products with the bruto formula Pro-Glc_{10}. Minor quasi-molecular ions $[M+K]^+$ at *m/z* 2325.8 and *m/z* 2974.0, corresponding to products with the bruto formulae Pro-Glc_{14} and Pro-Glc_{18}, respectively, were also present. The saccharide mixture was subjected to Bio-Gel P-2 chromatography, and two major fractions F and G each containing transfer products were isolated for further analysis. The MALDI-TOF mass spectra of fractions F and G showed a quasi-molecular ion $[M+Na]^+$ at *m/z* 2325.8, corresponding to the product Pro-Glc_{14}, and a quasi-molecular ion $[M+Na]^+$ at *m/z* 1661.5, corresponding to the product Pro-Glc_{10}, respectively (data not shown).

As a typical example, the 1D ^{1}H NMR spectrum of the Pro-Glc_{10}-containing fraction is depicted in Supplementary data, Figure S7. As already mentioned for the Lam-Glc_5 incubations, the group of anomeric signals **Gt** (δ 4.739), **Gi** (δ 4.785), **$G2_{\alpha/\beta}$** (δ 4.747, H-1_α / δ 4.765, H-1_β), **Gα/β** (δ 5.240, H-1α / δ 4.673, H-1β), **Gc** (δ 4.550) and **GD** (δ 4.753) indicated the presence of β-D-Glc*p*-(1→3)-, -(1→3)-β-D-Glc*p*-(1→3)-, -(1→3)-β-D-Glc*p*-(1→3)- (next to reducing-end **Gα/β**), -(1→3)-D-Glc*p*, -(1→3)-β-D-Glc*p*-(1→6)- and -(1→3,6)-β-D-Glc*p*-(1→3)- units, respectively (Table I) (Hreggvidsson et al. 2011). The same set of signals was found for the Pro-Glc_{14}-containing fraction. Integration of the well-resolved anomeric signals **Gc**, **Gα/β**, and the overlapping anomeric signals **Gi**, **GD**, **Gt**, **$G2_{\alpha/\beta}$** indicated that Pro-Glc_{10} contains one branching point [peak area ratio **Gα/β:Gc:(Gi,GD,Gt,G2)** = 1:1:8] and Pro-Glc_{14} two branching points [peak area ratio **Gα/β:Gc:(Gi,GD,Gt,G2)** = 1:2:11].

Based on the obtained MS and one- and two-dimensional NMR data of Pro-Glc_{10} and Pro-Glc_{14}, combined with the detailed data collected for the isomeric oligosaccharides obtained from the Lam-Glc_5/Glt20 incubation and the fact that oligosaccharide-alditols are not substrates for the Glt20 enzyme, taking into account the discussion on the Pro-Glc_8 and Pro-Glc_{11} isomeric structures (Lam-Glc_5/Glt20 incubation), it is hypothesized that Pro-Glc_{10} and Pro-Glc_{14} are synthesized by a transfer of a β-D-Glc*p*-(1→3)-β-D-Glc*p*-(1→3)-β-D-Glc*p*-(1→3)-β-D-Glc*p* tetrasaccharide unit from the non-reducing end of a donor Lam-Glc_6 substrate to the third, fourth or fifth internal Glc residue of an acceptor Lam-Glc_6 substrate via an O-3→O-6 transition, thereby

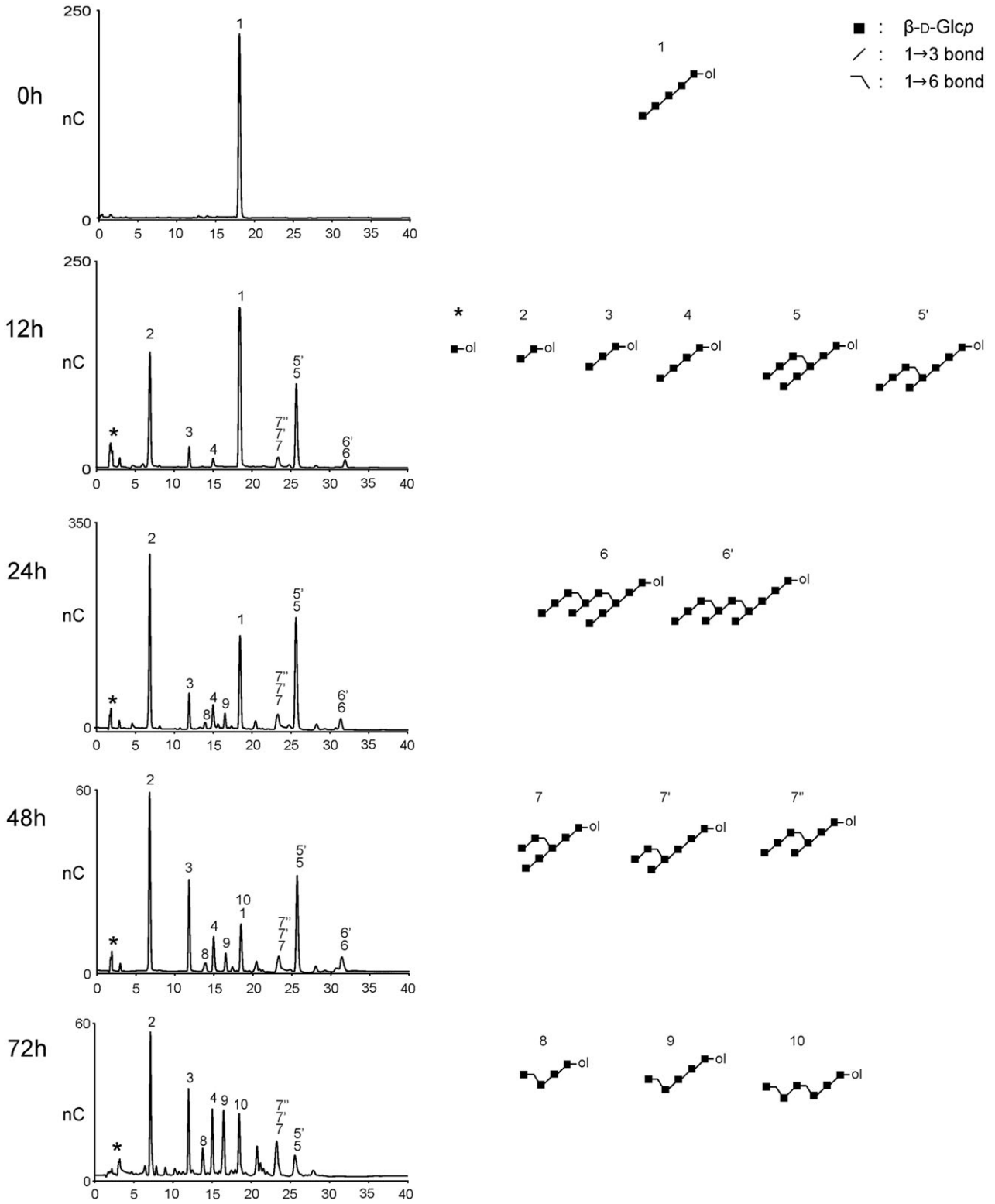

Fig. 7. HPAEC-PAD profile (0 to 500 mM NaOAc gradient in 100 mM NaOH) on CarboPac PA-1 of the oligosaccharide-alditol mixture obtained via incubation of Lam-Glc_5 with the Glt20 enzyme at $t = 0$, 12, 24, 48, 72 h (pH 6.5, 30°C) and subsequent reduction with $NaBH_4$. Established oligosaccharide structures for isolated fractions are included. Glucitol has been indicated with *. In view of the working up procedure, part of the glucitol is lost.

releasing laminaribiose (first branching, yielding three Pro-Glc_{10} isomeric structures). Following the "Lam-Glc_5 reasoning" described above, this reaction is followed by a second O-3→O-6 tetrasaccharide transfer to create the second branching product (Pro-Glc_{14}), and then the third branching product (Pro-Glc_{18}). The following structures are possible for Pro-Glc_{10} and Pro-Glc_{14}:

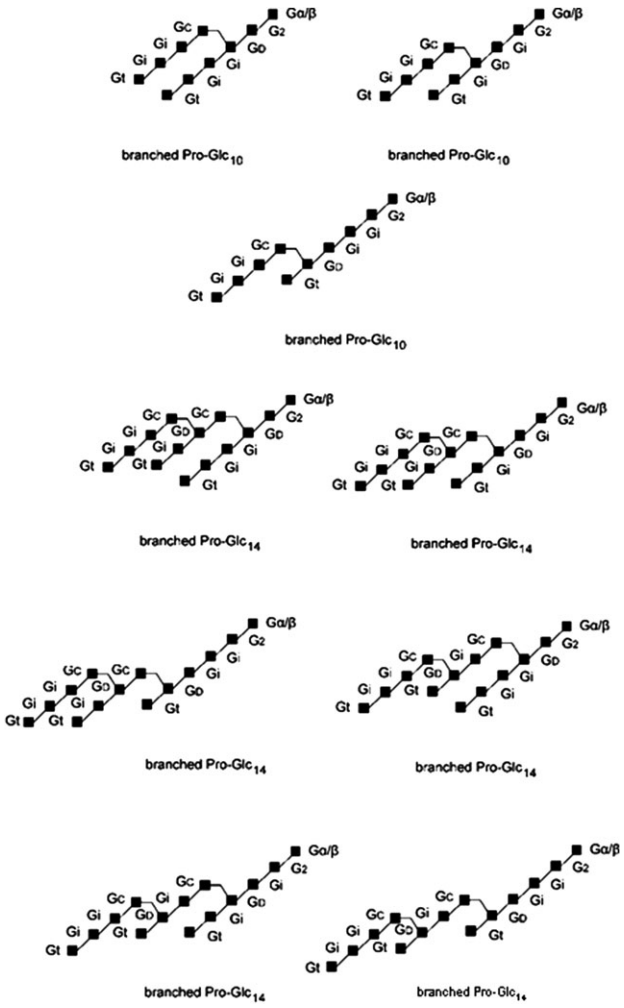

As was observed earlier, the hydrolytic activity of Glt20 increased with prolonged (72 h) incubation. This results in removal of terminal β-D-Glc*p*-(1→3)- residues ultimately leading to linear structures (data not shown).

Discussion

Bioinformatics analysis of bacterial genomes shows that bacterial GH17 enzymes are mostly confined to the phyla of *Proteobacteria* and *Bacteroidetes*. In contrast to the *Bacteroidetes* enzymes, the GH17 enzymes of *Proteobacteria* appear to be part of membrane bound proteins. Insertional inactivation of GH17 genes in *B. diazoefficiens* and *P. aeroginosa* has shown that the corresponding enzyme products participate in the formation of OPGs (Bhagwat and Keister 1995; Bhagwat et al. 1996; Sadovskaya et al. 2010).

Recently, three GH17 enzymes, Glt1, Glt3 and Glt7, from the proteobacteria *P. aeruginosa, P. putida* and *A. vinelandii,* respectively, were produced in *E. coli* and characterized. These GH17 enzymes form one of two structural domains of apparent membrane bound proteins, the other domain being a GT2 glycosyl transferase. The recombinant proteins were explored regarding the ability to modify linear (β1→3)-linked gluco-oligosaccharides (Hreggvidsson et al. 2011).

In the current work, an additional GH17 protein, part of the *ndvB* gene product in *B. diazoefficiens* (Glt20), was studied. Glt20 was recombinantly produced as fusion protein (designated Glt20-MalE) with a N-terminal maltose binding protein (MalE). MalE could be separated from the Glt20 domain by highly specific proteolytic cleavage using a recombinant ULP protease targeting a Smt3 site between the fusion tag and the GH17 domain (Motejadded and Altenbuchner 2009). The MalE domain, as a fusion partner, is known to affect properties of fusion proteins (Kale et al. 2015). For this reason, the Glt20-MalE enzyme was characterized parallel to Glt20 using (β1→3)-linked gluco-oligosaccharides (laminari-oligosaccharides; Lam-$Glc_{2\text{-}10}$). This was considered important, because if MalE would have no significant impact on the enzyme properties, a step involving cleavage from MalE and subsequent purification could be omitted for downstream enzyme applications. The results obtained for the incubations with the Glt20-MalE protein have been included in the Supplementary data.

As for Glt20, the Glt20-MalE enzyme was only active on Lam-$Glc_{5\text{-}10}$ substrates, not on Lam-$Glc_{2\text{-}4}$ substrates. Both enzymes were inactive on all corresponding alditol Lam-$Glc_{2\text{-}10}$-ol substrates. When incubated for 48 h, in case of the Lam-$Glc_{5\text{-}10}$ substrates (acting as donor and acceptor substrates), they catalyze the release of a laminaribiose unit from the reducing end of the donor substrates and transfer the remaining oligosaccharide part (tri- up to octa-saccharides depending on the substrate used) to the acceptor substrates in a first cycle. The transfer involves a (β1→3) → (β1→6) transition, resulting in branched structures [-(1→3,6)-β-D-Glc*p*-(1→3)-], as worked out in detail for Lam-Glc_5 (→Pro-Glc_8). In the second cycle the isomeric structures formed (for Lam-Glc_5: Pro-Glc_8 →Pro-Glc_{11}) are used as new acceptor substrates, following the same rules for oligosaccharide transfer as seen for the first cycle. This can even be followed by a third cycle (for Lam-Glc_5: Pro-Glc_{11} → Pro-Glc_{14}). The predicted schematic transglycosylation mechanism for the Glt20 enzyme, according to the detailed product analysis described in this paper, is shown in Figure 8A and B.

With Glt20-MalE, the (β1→3) → (β1→6) oligosaccharide transfer also occurs onto the terminal end of the acceptor substrates [-(1→6)-β-D-Glc*p*-(1→3)-], thereby creating kinked, linear structures (see Supplementary data). Lam-Glc_6 as a substrate results in a more complex mixture of compounds. Clearly, at higher DP values more complex mixtures of branched and kinked, linear oligosaccharides are formed. Even structures containing both branched and kinked elements cannot be excluded. It can also be concluded that the N-terminal MalE interferes with the binding of the larger oligosaccharides due to steric hindrance thereby affecting the enzymatic product formation.

Prolonged incubation time changed the composition of the oligosaccharide mixture (Figure 8B). As shown for Lam-Glc_5 and Lam-Glc_6, the formation of the single, double and triple branched and kinked oligosaccharides is optimal up to 48 h. After 72 h of incubation, when all the primary substrate is depleted, the branched and kinked products were hydrolyzed into linear products, containing internal or terminal (β1→6) linkages. This indicates that the transferase reaction is highly preferred over the hydrolysis reaction: the latter only becoming significant after depletion of the donor substrate. β-1,3-Glucosidase activity has not been described for native *E. coli* BL21 host cells and no indication of co-purified β-1,3-glucosidase was observed. Furthermore, Glt20 and Glt20-MalE enzymes revealed no activity on laminari-oligosaccharide-alditols even after 72 h of incubation. Hence, contamination by an exo/endo-β-glucosidase can be excluded.

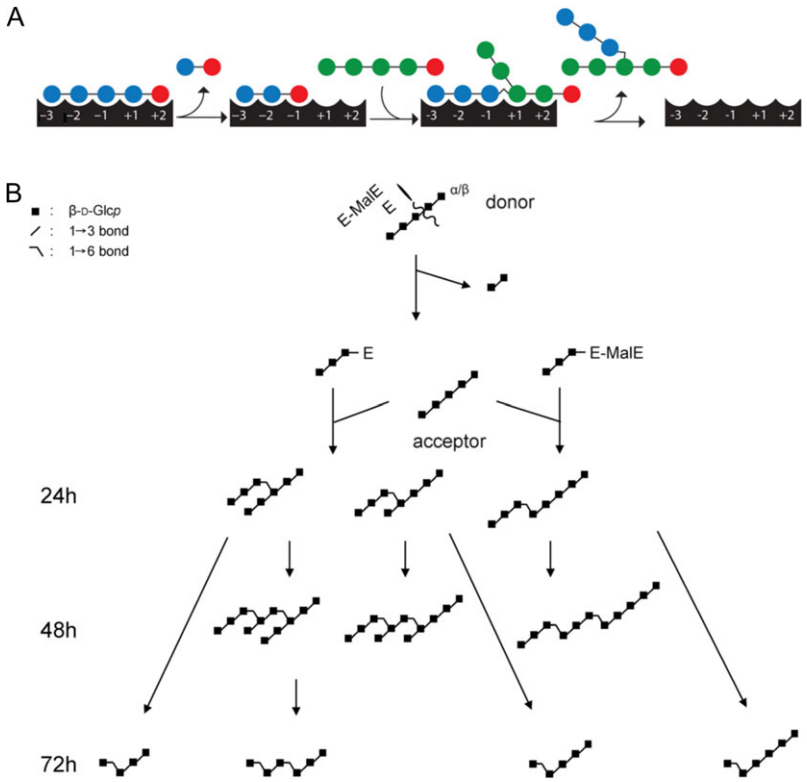

Fig. 8. Predicted schematic transglycosylation mechanism proposed for Glt20 based on the product analysis described for Lam-Glc_5 (A). The reducing end of both donor and acceptor is indicated in red. Otherwise, the donor substrate is in blue and the acceptor in green. Catalytic reactions occur between the −1 and +1 sub-sites of the enzyme. The Glt20 enzyme cleaves donor laminari-oligosaccharide substrates two glucose moieties from the reducing end, releasing laminaribiose and transferring the remainder to laminari-oligosaccharide acceptor substrates creating only (β1→6) linkage between the reducing end of the donor and the second or the third moiety of the acceptor from the non-reducing end. In the drawing, the branching is indicated with an elbow line, occurring three moieties from the non-reducing end of the acceptor. The scheme below (B) indicates the enzyme reaction (Glt20 and Glt20-MalE) using Lam-Glc_5 as substrate. Only major structures are included. This figure is available in black and white in print and in colour at *Glycobiology* online.

According to the results presented in this paper, the activity of the Glt20 enzyme is remarkably different from the other bacterial GH17 enzymes investigated so far: The Glt1, Glt3 and Glt7 enzymes cleave short (β1→3)-linked gluco-oligosaccharide fragments from the non-reducing end (Hreggvidsson et al. 2011), but the Glt20 enzyme cleaves from the reducing end, just like the secreted branching GH17 enzymes from the fungi *C. albicans* and *A. fumigatus* (Hartland et al. 1991; Gastebois et al. 2010). This may be of significant interest with respect to investigating the structure-function relationship of this enzyme family. The crystal structure of a novel GH17 β-1,3-glucanosyltransferase from the fungi *Rhizomucor miehei* was newly described. The structure explains the catalytic mode of this enzyme, in which laminaribiose is released from the reducing end of a linear (β1→3)-glucan and the remaining glucan is transferred to the end of another (β1→3)-glucan acceptor (Qin et al. 2015). The transfer/hydrolysis ratio of the Glt20 enzyme on laminari-oligosaccharides was very high compared with the Glt1, Glt3 and Glt7 enzymes and unlike them, it had no activity on derived alditols.

Synthesis of cyclic β-glucans by *Bradyrhizobium* species and their composition and biological function have been thoroughly studied (Miller et al. 1990; Tully et al. 1990; Rolin et al. 1992; Bhagwat and Keister 1995; Bhagwat et al. 1996, 1999; Choma and Komaniecka 2011). Although formation of cyclic structures could be excluded in our detailed studies on Lam-Glc_5 and Lam-Glc_6, the capability of Glt20 to cleave linear oligosaccharides from the reducing end should enable cyclization of long glucan chains. This ability of Glt20 corroborates results of previous studies on cyclic β-glucan from native *Bradyrhizobium* species (Rolin et al. 1992; Bhagwat and Keister 1995; Choma and Komaniecka 2011) and indicates its biological significance. The present study shows that Glt20 forms (β1→6) linkages and would therefore be expected to close the cycles with a (β1→6) linkage. This is in contrast to the cyclic structure of the β-glucan from the *B. diazoefficiens ndvC* mutant, proposed by Bhagwat et al. (1999) and Pfeffer et al. (1996), which only had (β1→3) linkages and a branch of two glucose moieties attached to the cycle with a (β1→6) linkage. According to the present study, the cyclic β-glucan from *B. diazoefficiens ndvC* mutant should contain one internal (β1→6) linkage generated with the cyclization of (β1→3) glucan chains by Glt20.

Synthesis of cyclic structures such as proposed by Rolin et al. (1992) and Bhagwat et al. (1999) may be a complex process requiring involvement of other biocatalytic entities such as the GT2 domain fused to Glt20 in NdvB, and NdvC, which is a membrane protein with a single GH17 domain. Our observations on the enzyme properties are based on in vitro experiments using oligosaccharides as substrates. The experiments are not reflecting biological conditions or the in vivo function of the enzyme participating in the synthesis of larger cyclic glucans. Moreover, the capability of Glt20 to form cyclic oligomers could not be tested, as laminari-

oligosaccharides DP >7 are not commercially available. Therefore, we cannot make any conclusion on the biological function of Glt20 based on the data on the transglucosidase activity as well as the hydrolase activity observed after prolonged incubation of the enzyme (72 h). However, the hydrolyzing activity may be explained by its function in releasing of the cycle after formation. One can visualize formation of a long linear β-glucan chain by the two domain protein (GH17-GT2), which after having reached a certain size, is available for cyclization by (β1→6) linkage formation to the reducing end. This could consequently make a conformational change activating the hydrolyzing property of the enzyme to release the ring. Therefore, the GH17 enzyme may have an endo-hydrolyzing activity evoked by structural changes of the β-glucan chain.

Numerous publications have reported diverse bioactivities of (β1→3)-glucans including immunomodulary, anti-tumoral, anti-infectious activities and protection against fungi, bacteria and virus infections (Zekovic et al. 2005; Chen and Seviour 2007; Mantovani et al. 2008; Bădulescu et al. 2009; Chan et al. 2009; Stier et al. 2014). These activities appear to be dependent on conformational complexity, linkage composition, degree of branching, degree of polymerization, conformation, solubility and molecular weight (Yadomae and Ohno 1996; Kim et al. 2000).

Heterogeneous natural extracts have proven to be less effective than purified β-glucan fractions, but purification of potent β-glucan fractions is difficult and expensive (Vetvicka and Vetvickova 2010; Saraswat-Ohri et al. 2011). With appropriate enzymes as described in this paper, potent tailor-made β-glucans can be produced for specific food and pharmaceutical applications. More complex structures, mixed linkage and/or highly branched, cyclic or linear β-glucans could potentially be engineered from inexpensive and more simple β-glucan polysaccharide substrates, e.g. from baker's yeast glucans or laminarin found in relatively large quantities in brown algae. Availability of (β1→3)(β1→6)-glucan oligosaccharides with defined structures and bioactive properties would extend the application range. Oligosaccharides could be used in functional food products without causing drastic changes in texture (e.g. beverages), in contrast to the more viscous β-glucan polysaccharides. Furthermore, a number of roles depending on functional activities and physical properties such as size, complexity and other structural features of β-glucans, oligo- or polysaccharides, can be envisaged in the cosmetic industry.

Materials and methods

Bacterial strains, plasmids and growth conditions

E. coli BL21 C43 (Dumon-Seignovert et al. 2004) was used as host for the cloning and the production of the recombinant Glt20 enzyme. *E. coli* strains carrying the cloned *glt20* gene were grown in LB medium supplemented with 100 µg/mL ampicillin. The expression vector pJOE4905 was used for the cloning experiments (Motejadded and Altenbuchner 2009).

Recombinant enzymes and DNA techniques

Recombinant DNA techniques, such as plasmid DNA preparations, cloning and agarose gel electrophoresis were performed according to conventional protocols (Sambrook et al. 1989). Genomic DNA was extracted applying the NucleoSpin Tissue kit from Macherey-Nagel (Düren, Germany) according to instructions of the manufacturer. Restriction enzymes were purchased from New England BioLabs (Hichin, Hertfordshire, UK) and used as recommended by the manufacturer. Pfx PCR polymerase was purchased from Invitrogen (Taastrup, Denmark). The Gel extraction Kit, GFX^{TM} PCR DNA and Gel Band Purification Kit were purchased from GE Healthcare (Uppsala, Sweden).

Cloning and expression of the *glt20* gene in *E. coli*

The reference gene sequence encoding the GH17 domain of NdvB from *B. diazoefficiens* USDA 110 is available in the NCBI GenBank database (http://www.ncbi.nlm.nih.gov/gene/) under the accession number AF047687.1. The sequence encoding the GH17 domain, excluding a 46 bp 5′ signal peptide encoding sequence, was synthesized artificially by Eurofins MediGenomix GmbH (Ebersberg, Germany) with *E. coli* codon usage adaptation. The C-terminal boundary of the GH17 domain was set upstream of a transmembrane helices region separating the GH17 and the GT2 glucosyltransferase domains, predicted according to sequence alignment and modelling (data not shown). The synthesized gene sequence, designated *glt20*, is available in the NCBI GenBank database (http://www.ncbi.nlm.nih.gov/gene/) under the accession number: KU043394. The *glt20* sequence was amplified from the plasmid carrying the synthesized gene by PCR with a proof reading polymerase (Platinum Pfx from Invitrogen); and the primers Glt20-f: 5′GCCAGCAAGGGCGAGATGGCAGGTTATGGGGG3′ and Glt20-r: 5′GCCCAAGCTTA TTCAACCGGACCTGTCCA3′. The amplified fragment was cut with *HinDIII* and ligated into *SfoI* – *HinDIII* digested pJOE4905 vector, resulting in fusion of the GH17 encoding sequence with a short 5′ linker sequence encoded within the primer, in-frame with the plasmid encoding maltose binding domain MalE, a 6xHis-tag and a Smt3 ubiquitin-like protein sequences (Motejadded and Altenbuchner 2009). *E. coli* BL21 C43 was transformed with the ligation product using an electrotransformation protocol (Jacobs et al. 1990). Correct sequence and fusion were verified by sequence analysis. Expression was carried out by growing the *E. coli* BL21 C43 *glt20* clone in LB medium with ampicillin at 37°C until the growth reached an optical density value (OD_{600}) of 0.8. Then, L-rhamnose was added to the culture medium (end concentration 0.1%) for induction. Subsequently, the clones were cultivated overnight at 25°C. The cells were harvested by centrifugation, suspended in buffer consisting of 20 mM Tris, pH 7.6 and disrupted by sonification. The soluble fraction was separated from the insoluble fraction by centrifugation. Expression of recombinant proteins was analyzed by running cleared samples of supernatant and insoluble fractions on SDS-PAGE.

Purification and separation of Glt20 from the MalE domain

The purification and separation of Glt20 from the MalE domain was performed according to a previously described protocol (Motejadded and Altenbuchner 2009) with some modifications. Briefly, before loading on a TriconTM 10/50 column (GE Healthcare), packed with amylose resin EB021S (New England Biolabs) according to the instructions of the manufacturer, the supernatant was filtrated through a 0.45-µm filter (Millipore, Billerica, MA). The binding buffer consisted of 20 mM Tris, pH 7.6, containing 200 mM NaCl and the elution buffer of 20 mM Tris, pH 7.6, containing 200 mM NaCl and 10 mM maltose. The column was run at a flow rate of 0.8 mL/min. The concentration of the elution buffer was increased linearly (0–100%) over five column volumes. Three elution fractions containing the majority of the

MalE-6xHis-Smt3-Glt20 (designated Glt20-MalE) fusion protein were combined. Then, the MalE domain was separated from the Glt20 protein by incubating 1 μg ULP protease with 1 mL of the combined fractions for 4 h at 30°C. Following the separation, the sample was desalted on a 5-mL HiTrap Sephadex G-25 desalting column (GE Healthcare), using HisTrap binding buffer consisting of 20 mM sodium phosphate, pH 7.6, containing 500 mM NaCl and 10 mM imidazole. The sample was applied on a 5-mL HisTrapFF chelating column charged with 0.5 mL 0.1 M $NiSO_4$ (GE Healthcare), and the flow through was collected in fractions of 1 mL. Two fractions were combined and desalted on a 5-mL HiTrap desalting column into a storage buffer of 20 mM sodium phosphate, pH 7.0, containing 150 mM NaCl. Protein contents were assayed using Bradford reagent (BioRad, Hercules, CA) with bovine serum albumin (Sigma, St. Louis, MO) as standard. The purity of Glt20 in the eluates was evaluated by running them on 10% SDS-PAGE gels with molecular-mass-marker proteins in the range 2–212 kDa (New England Biolabs); the gels were stained with Coomassie protein reagent (Sigma).

Laminari-oligosaccharides(-alditols)

Laminari-oligosaccharides [linear (β1→3)-gluco-oligosaccharides] of DP2-DP7, purchased from Megazyme (Bray, Ireland) (Lam-Glc_{2-6}) and Seikagaku Corp. (Tokyo, Japan) (Lam-Glc_7), were purified by size-exclusion chromatography on Bio-Gel P-2. Furthermore, laminari-oligosaccharides of DP2-DP10 (Lam-Glc_{2-10}) were prepared by partial acid hydrolysis of curdlan (from *Alcaligenes faecalis*; Fluka, Buchs, Switzerland), purified and eventually reduced with $NaBH_4$ to yield oligosaccharide-alditols (Hreggvidsson et al. 2011).

Enzyme assays and isolation of products

The (β1→3)-gluco-oligosaccharides(-alditols) [Lam-Glc_{2-10}(-ol)] were incubated individually with the Glt20 and Glt20-MalE enzymes in 0.5 M phosphate buffer, pH 6.5, at 30°C. In analytical experiments 100 μL oligosaccharide(-alditol) (6.25 mg/mL) was mixed with 30 μL 0.5 M phosphate buffer, pH 6.5 and 70 μL enzyme (1.0 mg/mL). The progress of the reaction (0–72 h) was followed by analyzing aliquots of the reaction mixture on TLC (Merck Kieselgel 60 F254 sheets; butanol:acetic acid:water = 2:1:1; orcinol/sulfuric acid staining).

Product mixtures of free oligosaccharides obtained directly after reaction in semi-preparative-scale experiments were fractionated on a Bio-Gel P-2 column (90 × 1 cm), eluted with 10 mM NH_4HCO_3 at a flow rate of 12 mL/h. Fractions of 5 min were collected and analyzed by TLC. Fractions containing oligosaccharides (DP > substrate) were used for further studies.

Product mixtures of oligosaccharide-alditols, obtained after reduction of part of the free oligosaccharide reaction mixtures with $NaBH_4$ (completeness of the reduction was checked by ^1H NMR analysis), were fractionated by HPAEC on a Dionex DX500 workstation (Dionex, Amsterdam, The Netherlands). The instrument was equipped with a CarboPac PA-1 column (Dionex; 250 × 4 mm for analytical runs, 250 × 9 mm for preparative runs) and an ED40 pulsed amperometric detector (PAD), and a linear gradient of 0–500 mM sodium acetate in 100 mM NaOH was applied. Collected fractions were immediately neutralized with 4 M acetic acid, desalted on CarboGraph SPE columns (Alltech, Breda, The Netherlands) using acetonitrile:water = 1:3 as eluent, and lyophilized.

Mass spectrometry

MALDI-TOF-MS experiments were performed using an Axima^{TM} mass spectrometer (Shimadzu Kratos Inc., Manchester, UK) equipped with a nitrogen laser (337 nm, 3 ns pulse width). Positive-ion mode spectra were recorded using the reflector mode at a resolution of 5000 FWHM and delayed extraction (450 ns). The accelerating voltage was 19 kV with a grid voltage of 75.2%. The mirror voltage ratio was 1.12 and the acquisition mass range was 200–6000 Da. Samples were prepared by mixing on the target 0.5 μL sample solutions with 0.5 μL aqueous 10% 2,5-dihydroxybenzoic acid as matrix solution.

NMR spectroscopy

Resolution-enhanced one- and two-dimensional NMR spectra were recorded in D_2O on a Bruker DRX-500 spectrometer (NMR Spectroscopy, Bijvoet Center, Utrecht University, The Netherlands) at a probe temperature of 335 K. Prior to analysis, samples were exchanged twice in D_2O (99.9 atom% D, Cambridge Isotope Laboratories, Inc., Andover, MA) with intermediate lyophilization, and then dissolved in 0.6 mL D_2O. Suppression of the HOD signal was achieved by applying a water-eliminated Fourier transform (WEFT) pulse sequence for one-dimensional NMR experiments and by a pre-saturation of 1 s during the relaxation delay in two-dimensional experiments. The two-dimensional TOCSY spectra were recorded using an MLEV-17 mixing sequence with spin-lock times of 40–200 ms. The two-dimensional ROESY spectra were recorded using standard Bruker XWINNMR software with mixing time of 200 ms. The carrier frequency was set at the downfield edge of the spectrum in order to minimize TOCSY transfer during spin-locking. Natural abundance two-dimensional ^{13}C-^1H HSQC experiments were recorded without decoupling during acquisition of the ^1H FID. Resolution enhancement of the spectra was performed by a Lorentzian-to-Gaussian transformation for one-dimensional spectra or by multiplication with a squared-bell function phase shifted by π/(2.3) for two-dimensional spectra, and when necessary, a fifth order polynomial baseline correction was performed. Chemical shifts (δ) are expressed in ppm by reference to internal acetone (δ 2.225 for ^1H and δ 31.07 for ^{13}C).

Supplementary data

Supplementary data for this article are available online at http://glycob.oxfordjournals.org/.

Funding

The work was supported by EU FP7 grant 265992 AMYLOMICS and the Icelandic Research Fund grants, 70209021 and 141341-052.

Acknowledgements

We are grateful to Sólveig Ólafsdóttir, Lilja B. Jónsdóttir, Brynjar Ö. Ellertsson and Ingunn Jónsdóttir for providing technical support.

Conflict of interest statement

None declared.

Abbreviations

DP, degree of polymerization; FID, free induction decay; HSQC, heteronuclear single quantum coherence; MALDI-TOF-MS, matrix-assisted laser-desorption ionization time-of-flight mass spectrometry; MLEV, composite pulse devised by M. Levitt; NMR, nuclear magnetic resonance; OPG, osmoregulated periplasmic glucan; ROESY, rotating-frame nuclear Overhauser enhancement spectroscopy; SDS, sodium dodecyl sulfate; TLC, thin-layer chromatography; TOCSY, total correlation spectroscopy; WEFT, water-eliminated Fourier transform.

References

Bădulescu MM, Apetrei NS, Lupu AR, Cremer L, Szegli G, Moscovici M, Mocanu G, Mihai D, Călugăru A. 2009. Curdlan derivatives able to enhance cytostatic drugs activity on tumor cells. *Roum Arch Microbiol Immunol*. 68(4):201–206.

Bhagwat AA, Keister DL. 1995. Site-directed mutagenesis of the β-(1→3), β-(1→6)-D-glucan synthesis locus of *Bradyrhizobium japonicum*. *Mol Plant Microbe Interact*. 8(3):366–370.

Bhagwat AA, Gross KC, Tully RE, Keister DL. 1996. β-Glucan synthesis in *Bradyrhizobium japonicum*: Characterization of a new locus (*ndvC*) influencing β-(1→6) linkages. *J Bacteriol*. 178(15):4635–4642.

Bhagwat AA, Mithöfer A, Pfeffer PE, Kraus C, Spickers N, Hotchkiss A, Ebel J, Keister DL. 1999. Further studies of the role of cyclic β-glucans in symbiosis. An *ndvC* mutant of *Bradyrhizobium japonicum* synthesizes cyclodecakis-(1→3)-β-glucosyl. *Plant Physiol*. 119(3):1057–1064.

Bohin J-P. 2000. Osmoregulated periplasmic glucans in Proteobacteria. *FEMS Microbiol Lett*. 186(1):11–19.

Chan GC-F, Chan WK, Sze DM-Y. 2009. The effects of β-glucan on human immune and cancer cells. *J Hematol Oncol*. 2(6):25.

Chen J, Seviour R. 2007. Medicinal importance of fungal β-(1→3), (1→6)-glucans. *Mycol Res*. 111(6):635–652.

Choma A, Komaniecka I. 2011. Characterization of cyclic β-glucans of *Bradyrhizobium* by MALDI-TOF mass spectrometry. *Carbohydr Res*. 346(13):1945–1950.

Cogez V, Talaga P, Lemoine J, Bohin J-P. 2001. Osmoregulated periplasmic glucans of *Erwinia chrysanthemi*. *J Bacteriol*. 183(10):3127–3133.

Delamuta JR, Ribeiro RA, Ormeño-Orrillo E, Melo IS, Martínez-Romero E, Hungria M. 2013. Polyphasic evidence supporting the reclassification of *Bradyrhizobium japonicum* group Ia strains as *Bradyrhizobium diazoefficiens* sp. nov. *Int J Syst Evol Microbiol*. 63(9):3342–3351.

Dumon-Seignovert L, Cariot G, Vuillard L. 2004. The toxicity of recombinant proteins in *Escherichia coli*: A comparison of overexpression in BL21 (DE3), C41(DE3), and C43(DE3). *Prot Expr Purif*. 37(1):203–206.

Gastebois A, Mouyna I, Simenel C, Clavaud C, Coddeville B, Delepierre M, Latgé J-P, Fontaine T. 2010. Characterization of a new β(1-3)-glucan branching activity of *Aspergillus fumigatus*. *J Biol Chem*. 285(4):2386–2396.

Goldman RC, Sullivan PA, Zakula D, Capobianco JO. 1995. Kinetics of β-1,3 glucan interaction at the donor and acceptor sites of the fungal glucosyltransferase encoded by the *BGL2* gene. *Eur J Biochem*. 227(1–2):372–378.

Hartland RP, Emerson GW, Sullivan PA. 1991. A secreted β-glucan-branching enzyme from *Candida albicans*. *Proc Royal Soc Lond B*. 246(1316):155–160.

Hreggvidsson GO, Dobruchowska JM, Fridjonsson OH, Jonsson JO, Gerwig GJ, Aevarsson A, Kristjansson JK, Curti D, Redgwell RR, Hansen C-E et al. 2011. Exploring novel non-Leloir β-glucosyltransferases from proteobacteria for modifying linear (β1→3)-linked gluco-oligosaccharide chains. *Glycobiology*. 21(3):304–328 /revision 21(5):664-688.

Jacobs M, Wnendt S, Stahl U. 1990. High-efficiency electro-transformation of *Escherichia coli* with DNA from ligation mixtures. *Nucleic Acids Res*. 18 (6):1653.

Kale V, Fridjonsson O, Jonsson JO, Kristinsson HG, Omarsdóttir S, Hreggvidsson GO. 2015. Chondroitin lyase from a marine *Arthrobacter* sp. MAT3885 for the production of chondroitin sulfate disaccharides. *Mar Biotechnol*. 17(4):479–492.

Kim Y-T, Kim E-H, Cheong C, Williams DL, Kim C-W, Lim S-T. 2000. Structural characterization of β-D-(1→3, 1→6)-linked glucans using NMR spectroscopy. *Carbohydr Res*. 328(3):331–341.

Lequette Y, Rollet E, Delangle A, Greenberg EP, Bohin J-P. 2007. Linear osmoregulated periplasmic glucans are encoded by *opgGH* locus of *Pseudomonas aeruginosa*. *Microbiol*. 153(10):3255–3263.

Mah TF, Pitts B, Pellock B, Walker GC, Stewart PS, O'Toole GA. 2003. A genetic basis for *Pseudomonas aeruginosa* biofilm antibiotic resistance. *Nature*. 426(6964):306–310.

Mantovani MS, Bellini MF, Angeli JPF, Oliveira RJ, Silva AF, Ribeiro LR. 2008. β-Glucans in promoting health: Prevention against mutation and cancer. *Mut Res*. 658(3):154–161.

McIntosh M, Stone BA, Stanisich VA. 2005. Curdlan and other bacterial (1→3)-β-D-glucans. *Appl Microbiol Biotechnol*. 68(2):163–173.

Miller KJ, Gore RS, Johnson R, Benesi AJ, Reinhold VN. 1990. Cell-associated oligosaccharides of *Bradyrhizobium* spp. *J Bacteriol*. 172(1):136–142.

Motejadded H, Altenbuchner J. 2009. Construction of a dual-tag system for gene expression, protein affinity purification and fusion protein processing. *Biotechnol Lett*. 31(4):543–549.

Mouyna I, Hartland RP, Fontaine T, Diaquin M, Simenel C, Delepierre M, Henrissat B, Latgé J-P. 1998. A 1,3-β-glucanosyltransferase isolated from the cell wall of *Aspergillus fumigatus* is a homologue of the yeast Bgl2p. *Microbiology*. 144(11):3171–3180.

Mukhopadhyay P, Williams J, Mills D. 1988. Molecular analysis of a pathogenicity locus in *Pseudomonas syringae* pv. *syringae*. *J Bacteriol*. 170(12): 5479–5488.

Pfeffer PE, Osman SF, Hotchkiss A, Bhagwat AA, Keister DL, Valentine KM. 1996. Cyclolaminarinose. A new biologically active β-(1→3) cyclic glucan. *Carbohydr Res*. 296(1–4):23–37.

Qin Z, Yan Q, Lei J, Yang S, Jiang Z, Wu S. 2015. The first crystal structure of a glycoside hydrolase family 17 β-1,3-glucanosyltransferase displays a unique catalytic cleft. *Acta Crystallogr D Biol Crystallogr*. 71(8): 1714–1724.

Rolin DB, Pfeffer PE, Osman SF, Szwergold BS, Kappler F, Benesi AJ. 1992. Structural studies of a phosphocholine substituted β-(1,3);(1,6) macrocyclic glucan from *Bradyrhizobium japonicum* USDA 110. *Biochim Biophys Acta*. 1116(3):215–225.

Sadovskaya I, Vinogradov E, Li J, Hachani A, Kowalska K, Filloux A. 2010. High-level antibiotic resistance in *Pseudomonas aeruginosa* biofilm: The *ndvB* gene is involved in the production of highly glycerol-phosphorylated β-(1→3)-glucans, which bind aminoglycosides. *Glycobiology*. 20(7):895–904.

Sambrook J, Fritch EF, Maniatis T. 1989. *Molecular Cloning: A Laboratory Manual*, 2nd ed. New York, USA, Cold Spring Harbour Laboratory Press.

Saraswat-Ohri S, Vashishta A, Vetvicka V, Descroix K, Jamois F, Yvin J-C, Ferrières V. 2011. Biological properties of (1 → 3)-β-D-glucan-based synthetic oligosaccharides. *J Med Food*. 14(4):369–376.

Stier H, Ebbeskotte V, Gruenwald J. 2014. Immune-modulatory effects of dietary yeast beta-1,3/1,6-D-glucan. *Nutr J*. 13:38.

Talaga P, Fournet B, Bohin J-P. 1994. Periplasmic glucans of *Pseudomonas syringae* pv. *syringae*. *J Bacteriol*. 176(21):6538–6544.

Tully RE, Keister DL, Gross KC. 1990. Fractionation of the β-linked glucans of *Bradyrhizobium japonicum* and their response to osmotic potential. *Appl Environ Microbiol*. 56(6):1518–1522.

Vetvicka V, Vetvickova J. 2010. β1,3-Glucan: Silver bullet or hot air?. *Open Glycoscience*. 3:1–6.

Yadomae T, Ohno N. 1996. Structure-activity relationship of immunomodulating (1→3)-β-D-glucans. *Recent Res Dev Chem Pharm Sci*. 1:23–33.

Zekovic DB, Kwiatkowski S, Vrvic MM, Jakovljevic D, Moran CA. 2005. Natural and modified (1→3)-β-D-glucans in health promotion and disease alleviation. *Crit Rev Biotechnol*. 25:205–230.